



## Dynamic Fracture Initiation in Metals and Preliminary Results on the Method of Caustics for Crack Propagation Measurements

L. B. Freund

Chairman and Professor,  
Fellow ASME

J. Duffy

Professor,  
Fellow ASME

A. J. Rosakis

Research Assistant

Division of Engineering,  
Brown University,  
Providence, R.I.

*In the first part of this report, progress is described in the use of an experimental method for studying fracture initiation under dynamic loading conditions in metals. Loading rates in excess of  $\dot{K}_I = 10^6 \text{ MPa } \sqrt{\text{m}} \text{ s}^{-1}$  are attainable with this method, and the instrumentation provides unambiguous records of instantaneous average stress on the unfractured ligament and of instantaneous crack opening displacement. Results of tests on three steels are reported. In the second part, the application of the optical method of caustics is discussed for measuring fracture toughness during rapid crack propagation in metals. In this case, the procedure requires the use of light reflection from the deformed specimen surface. Known plane stress dynamic crack propagation solutions are used to estimate the influence of crack tip plasticity effects on the values of dynamic fracture toughness which are inferred for experimental data.*

### DYNAMIC FRACTURE INITIATION

In this section, an experimental procedure is described which was designed to determine quantitatively the influence of loading rate on fracture initiation resistance of metals. The procedure has been applied to obtain data on a number of steels over a range of temperatures. The data have been interpreted on the basis of standard fracture mechanics analysis and, following Krafft and Irwin [1] and others, the plastic flow properties of the materials which are required for data analysis are also measured under both quasi-static and dynamic conditions.

#### The Fracture Specimen and the Experimental Procedure

Dynamic fracture initiation experiments have been performed on an AISI 1018 cold rolled steel, a 1020 hot rolled steel, and a 4340 steel. The test consists of loading a notched round bar in tension by detonating an explosive charge at one end of the bar. The technique is described in detail in [2] and more briefly here; see Fig. 1. A circumferential notch is machined into a solid round bar, 2.54 cm in diameter and 112 cm in length, at a section 66 cm from the loading end. A circumferentially uniform fatigue crack is grown in from the

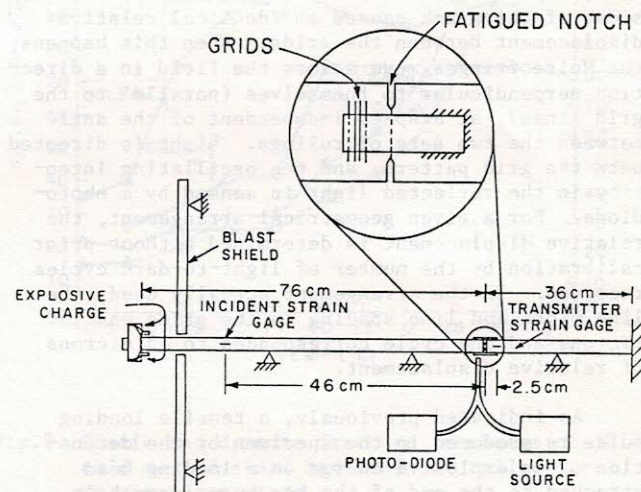


Fig. 1 Schematic of fracture initiation apparatus and specimen

root of the notch in a rotating bending apparatus, leaving an unfractured ligament with a diameter of about 1.25 cm. Loading of the precracked section is accomplished by a tensile stress pulse initiated at one end of the bar by the detonation of an explosive against a suitably shaped loading head which is bolted to the end of the bar.

The specimen is instrumented to obtain measures of the stress pulses which are incident on, reflected from, and transmitted through the precracked section. To perform these stress pulse measurements, two sets of strain gages are attached

to the specimen. The first set, called the incident gages, are placed 20 cm from the loading end of the bar. Their location is such as to be sufficiently far from the loading end to ensure that the transients induced by the explosion are not recorded, and far enough from the notch to ensure that the incident and reflected pulses may be recorded without mutual interference. The second set of gages, called the transmitter gages, are located 2.54 cm beyond the notch. These gages measure the stress pulse transmitted through the notched section. In his pressure bar experiments, Kolsky [3] showed that the transmitted pulse provides a direct measure of the average stress in the wafer specimen used. His observations may be applied to the fracture specimen to conclude that the magnitude of the transmitted pulse is directly proportional at each instant to the average net section stress at the fracture site. Further examination of the Kolsky pressure bar technique indicates that when the pulse length is long compared to the notch width the loading at the notched section may be viewed as being quasi-static for purposes of analysis. The transmitter gages are located close enough to the crack so that no significant amount of dispersion of the stress pulse has occurred at the measuring station, and yet far enough away to ensure uniaxial stress.

Accurate measurements of the crack opening displacement at the specimen surface are achieved by means of an optical extensometer based on the phenomenon of Moire fringes. Matched parallel-line grids are reproduced photographically on the specimen surface on one side of the crack and on an overlapping glass slide which is attached to the specimen surface on the other side of the crack. Thus, any relative displacement of the opposite sides of the crack causes an identical relative displacement between the grids. When this happens, the Moire fringes move across the field in a direction perpendicular to themselves (parallel to the grid lines), at a speed independent of the angle between the two sets of rulings. Light is directed onto the grid pattern, and the oscillating intensity in the reflected light is sensed by a photodiode. For a given geometrical arrangement, the relative displacement is determined without prior calibration by the number of light-to-dark cycles recorded. In the arrangement actually used, the line width and line spacing in the grids was 150 microns and one cycle corresponded to 15 microns of relative displacement.

As indicated previously, a tensile loading pulse is produced in the specimen by the detonation of an explosive charge on a loading head attached to the end of the bar by a large bolt. The rise time of the loading pulse as measured at the incident gages is about 20 to 25 microseconds. However, due to dispersion of the stress pulse as it propagates down the bar, the rise time of the pulse when it reaches the cracked section is 35 to 40 microseconds. Because fracture of the specimen normally occurs within 20 to 25 microseconds of the arrival of the loading pulse front, it is clear that fracture initiation occurs well within the rising portion of the loading pulse.

For the tests being described here, the instant of fracture initiation was determined from an analysis of the reflected pulse record. The onset

of crack growth produces a small but sudden increase in free surface area, and this results in an increase in the amplitude of the reflected pulse. In those tests in which the fracture mode was nominally brittle, it was found that fracture initiation was coincident with peak load on the cracked section. However, in those cases in which fracture initiation was preceded by significant amounts of plastic flow, crack growth began just before peak load was achieved at the cracked section of the specimen.

#### Analysis of Data

In each test the data recorded are in the form of oscilloscope traces. A common zero time point is established and an applied load versus crack opening displacement curve is generated for each test. Having determined the load-displacement curve, the fracture initiation parameters can be calculated. For a nominally brittle material the parameter of interest is  $K_{Ic}$ , the plane strain fracture toughness.  $K_{Ic}$  is calculated according to [4] as

$$K_I = \frac{P}{\pi R^2} \sqrt{\pi R} F(2R/D) \quad (1)$$

where  $R$  is the radius of the unfractured ligament,  $P$  is the applied load,  $D$  is the outer diameter of the bar, and  $F(2R/D)$  is a size function. For the specimen geometry described here the size function has a value of about 0.48. The load  $P$  used in calculating  $K_{Ic}$  from (1) is determined from the load-displacement curve in accordance with ASTM standards by using the 5% slope offset procedure. In order to apply linear fracture mechanics concepts, the size of the crack tip plastic zone must be small compared to the nominal dimensions of the specimen. As a criterion of a valid  $K_{Ic}$  test

$$R \geq 2.5(K_{Ic}/\sigma_y)^2 \quad (2)$$

is used, where  $\sigma_y$  is a flow stress of the material determined at a strain rate comparable to the strain rate achieved near the crack tip region during the fracture test. The required dynamic flow stresses were determined in shear by means of the Kolsky bar technique, as described in [5], on specimens cut from the fracture specimens.

When testing more ductile materials, the specimen size was inadequate to contain the plastic zone within the limit (2). In these cases, a J-integral approach was adopted. Paris [6] has suggested that a possible criterion for a valid  $J_{Ic}$  test is

$$R \geq 50 J_{Ic}/\sigma_y \quad (3)$$

This criterion was used in evaluating the validity of the results presented here. Rice, et al. [7] have shown that the value of  $J$  for a notched round bar may be determined from a load-displacement curve according to

$$J = \frac{1}{2\pi R^2} \left( 3 \int_0^{\delta_c} P d\delta_c - P\delta_c \right) \quad (4)$$

where  $\delta_c$  is the load-point displacement due to the presence of the crack. For present purposes, use of the crack opening displacement at the surface for the load point displacement was a good approximation. The key assumption in deriving (4) is that the radius  $R$  is the only specimen dimension of significance.

This assumption is valid as long as the plastic zones do not extend to the outer surface of the bar. Strictly speaking, the J-integral approach cannot be used for materials which exhibit significant amounts of subcritical crack growth prior to onset of instability, although a possible extension to materials of this type has been considered by Hutchinson and Paris [8].

A direct comparison can be made between the fracture parameters J and K by considering the specimen to be sufficiently large to be in the regime of linear elastic fracture mechanics. In such a case, J and K are related by

$$K^2 = \frac{EJ}{(1-\nu^2)} \quad (5)$$

where E is the elastic modulus and  $\nu$  is Poisson's ratio. Once a value of J is determined from an experiment, an equivalent  $K_{IC}^e$  may be calculated from (5), where  $K_{IC}^e$  has the interpretation as the value of the plane strain toughness which would have been measured had a large enough specimen been used.

Finally, the parameter used to specify the loading rate in the dynamic fracture test is

$$\dot{K}_I = K_{IC} / t_c \quad (6)$$

where  $t_c$  is the time required to increase the equivalent stress intensity factor from zero to the critical value  $K_{IC}$ .

## Results

The first results reported are for the AISI 4340 steel which, in the heat treated condition, has a static yield stress of 1400 MPa and which fractured in a nominally brittle manner. The chemical composition and heat treatment are given in [2]. The load-displacement curves for this material were nearly linear up to fracture initiation. A summary of results is shown in Table 1. The static tests

Table 1 Fracture Initiation Results for 4340 Steel

	$\dot{K}_I$	$K_{IC}$	$K_{IC}^e$	$J_{IC}$
	$MPa\sqrt{m} s^{-1}$	$MPa\sqrt{m}$	$MPa\sqrt{m}$	$kPa m$
Dynamic	$2 \times 10^6$	56	63	17.5
Static	1	63	62	16.5

to obtain the comparison data shown in Table 1 were performed in a standard testing machine using specimens exactly like those used in the dynamic tests. It is observed from the table that, while the loading rates for the dynamic and static tests differed by six orders of magnitude, there is essentially no difference between the fracture initiation resistance of the material under static and dynamic conditions. This is not entirely unexpected because the material response in bulk is essentially rate independent and the local separation is a deformation controlled ductile separation with void coalescence at an early stage due to void sheet formation.

Next, results are reported for 1018 cold rolled steel [9] and 1020 hot rolled steel [10]. The chemical compositions of the materials are given and details of the microstructures are described in the original references. These materials were tested at temperatures both above and below room temperature. During tests at temperatures other than ambient, the temperature was maintained using an environmental chamber which enclosed 15 cm of the specimen on either side of the notch. The low temperatures were reached by a controlled flow of liquid nitrogen which circulated throughout the chamber. The elevated temperatures were reached using electric heaters built into the chamber. A thermocouple was attached to the specimen just below the notched section. The specimens were maintained at the test temperature for at least 15 minutes prior to testing to ensure that thermal equilibrium was reached. In the dynamic plasticity tests to determine the dynamic plastic flow properties of the test materials, the temperature was controlled in a similar manner but with a slightly different apparatus.

The results of static and dynamic fracture toughness measurements on the 1018 and 1020 steels over a 300°C temperature range are shown in Fig. 2.

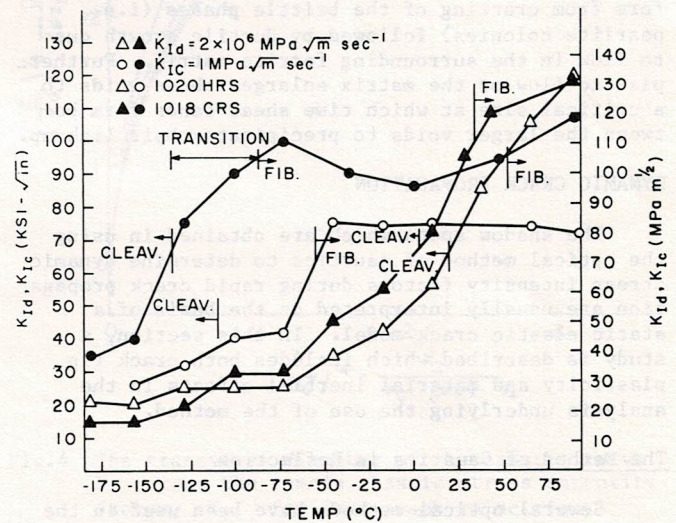


Fig. 2 Static and dynamic fracture toughness of 1018 cold rolled steel and 1020 hot rolled steel versus temperature

It is observed that the dynamic toughnesses of the two steels are nearly equal over the entire temperature range, and the temperature of transition to cleavage fracture differs by only about 20°C for the two materials. The static fracture curves for the two materials also exhibit similar general trends, but the hot rolled steel is substantially less fracture resistant than the cold rolled steel. A comparison of the static and dynamic curves for each steel in the region of cleavage fracture shows that fracture in the cold rolled steel is more strongly dependent on loading rate than in the hot rolled steel. This is in contrast to the apparent strain rate sensitivities determined in the dynamic plas-

ticity experiments in which the difference between dynamic and static flow stress is greater for the hot rolled than the cold rolled steel. In the temperature range where both static and dynamic fractures are fibrous, the sensitivity of fracture initiation to stress intensity factor rate tends to follow the same trend as the apparent strain rate sensitivity observed in the plasticity experiments. In this region the hot rolled steel dynamic toughness is greater than the static fracture toughness.

Examination of the fracture surfaces near the initiation sites shows that the mechanism of initiation is quite similar in the two materials. Below the transition temperature, transgranular cleavage occurs when a critical tensile stress is attained over a microstructural distance. For the cold rolled steel, which has a low strain hardening rate, results from preliminary models [11] are consistent with a picture of cleavage fracture of the ferrite grains following from cracks in grain boundary carbide platelets. For such a model, the characteristic microstructural distance becomes the mean spacing of carbide platelets, which was typically two to three grain diameters for the cold rolled steel tested. Because of the substantially higher strain hardening rate in the hot rolled steel, attempts at developing similar models have not been as successful. Ductile fracture in both steels proceeds by void nucleation. Voids seem to form from cracking of the brittle phases (i.e., pearlite colonies) followed by ductile growth due to flow in the surrounding ferrite matrix. Further plastic flow of the matrix enlarges these voids to a critical size at which time shear bands form between the larger voids to precipitate their link-up.

#### DYNAMIC CRACK PROPAGATION

The shadow spots which are obtained in using the optical method of caustics to determine dynamic stress intensity factors during rapid crack propagation are usually interpreted on the basis of a static elastic crack model. In this section, a study is described which includes both crack tip plasticity and material inertial effects in the analysis underlying the use of the method.

#### The Method of Caustics in Reflection

Several optical methods have been used in the past few decades to measure deformations in nominally elastic materials, and thereby to determine stress fields. Such methods have the advantage that they provide full field measurements rather than point observations, there is no coupling between the optical and mechanical fields, and the optical response is instantaneous on the time scale of mechanical response. Most of the techniques are based on light wave interference principles, and their application has been confined for the most part to transparent materials, or to opaque materials coated with transparent materials. Recently, the optical method of caustics, or the shadow spot method, was developed and applied in the investigation of nonuniform surface deformations due to stress concentrations in deformed solids [12]. Details of the stress field may then be inferred from shadow spot measurements on the basis of an analytical model of the physical system. The method of caustics is an exceptional procedure

because it is based on the principles of geometrical optics, rather than interference, and it has been successfully applied to both transparent and opaque materials.

The technique has been used in experiments involving rapid crack propagation and stress wave loading by Kalthoff and coworkers [13], Theocaris and coworkers [14], and Goldsmith and Katsamanis [15]. In each case, it was assumed that the elastic stress field near the tip of the rapidly growing crack in a brittle solid has precisely the same spatial variation as the elastic plane stress field near the tip of a stationary crack. More recently, several investigators have reanalyzed the method of caustics as applied to brittle materials, including the effect of inertia on the spatial variation of the elastic crack tip stress field [16,17]. It was found that, for some typical laboratory materials used in crack propagation studies, the neglect of inertia could lead to errors of up to 30% to 40% in the value of the stress intensity factor inferred from the measured caustic diameter.

A first attempt at including plasticity effects in the analysis underlying the method of caustics as applied in dynamic crack propagation studies is outlined here. The details may be found in [18]. The analysis is based on the theory of plane stress and the one dimensional plastic zone model of Dugdale and Barenblatt. For this analysis, consider a family of parallel light rays which are incident on the reflective surface  $x_3 = -f(x_1, x_2)$  of an opaque specimen as shown in Fig. 3. The light rays will deviate from parallelism upon reflection and,

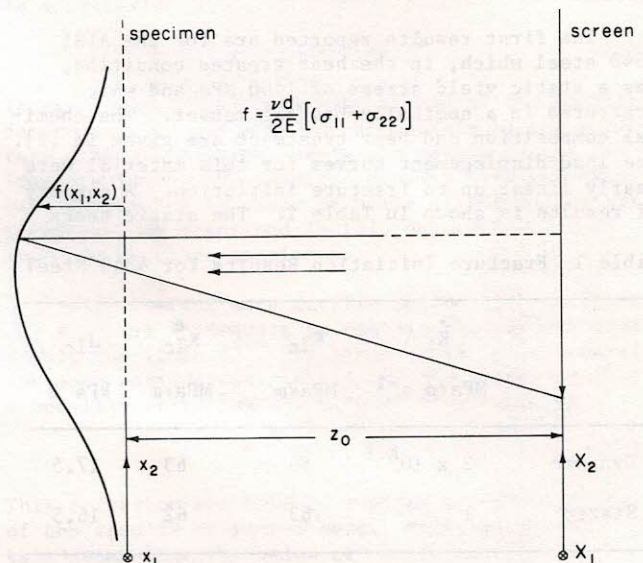


Fig.3 Diagram showing reflection of parallel light rays from a deformed specimen onto a screen

if certain geometrical conditions are met, the reflected rays will have an envelope in the form of a three dimensional surface in space. This surface, which is called the caustic surface, is the locus of points of maximum luminosity in the reflected field, and the reflected rays are tangent to the caustic surface. If a screen is positioned parallel to the specimen surface so that it intersects the caustic

surface, then a cross section of the caustic surface can be observed as a bright curve (the caustic curve) bordering a dark region (the shadow spot) on the screen. If  $z_0$  is the distance from the screen to the specimen, then the ray reflected from the specimen at point  $(x_1, x_2)$  intersects the screen at the point  $(X_1, X_2)$  where

$$X_i = x_i \pm 2z_0(\partial f / \partial x_i), \quad i = 1, 2 \quad (7)$$

The choice of sign in (7) depends on whether the image is real or virtual.

When the screen intersects a caustic surface, the resulting caustic curve on the screen is a locus of points of multiple reflection. That is, the mapping from the specimen surface to the screen is not invertible or

$$\text{Jacobian}(x_1, x_2) = \frac{\partial(X_1, X_2)}{\partial(x_1, x_2)} = 0 \quad (8)$$

The locus of points  $(x_1, x_2)$  on the specimen which satisfy (8) is called the initial curve, and the rays reflected from points on the initial curve form the caustic curve on the screen according to (7). Thus, the caustic curve may be predicted once the lateral contraction of the specimen  $f(x_1, x_2)$  is known from stress analysis. For plane stress deformation of a plate of uniform thickness  $d$  the lateral contraction is given by

$$f(x_1, x_2) = \nu d(\sigma_{11} + \sigma_{22})/2E \quad (9)$$

where  $\nu$  is Poisson's ratio,  $E$  is the elastic modulus, and  $\sigma_{11} + \sigma_{22}$  is the first stress invariant. For steady dynamic plane stress growth of a tensile crack under small scale yielding conditions which is accompanied by a one dimensional plastic zone of length  $R$  and uniform cohesive stress  $\sigma_0$ , the first stress invariant is given by

$$(\sigma_{11} + \sigma_{22}) = \frac{(1+\nu)\rho v^2 2\sigma_0 (2-\nu^2/c_s^2)}{\mu\pi Q} \text{Re} \left( \arctan \left( \frac{R}{z_l - R} \right)^{1/2} \right) \quad (10)$$

where  $\rho$  is the material mass density,  $v$  is the speed of crack growth,  $\mu$  is the elastic shear modulus, and

$$R = (\pi/8)(K_I/\sigma_0)^2 \quad z_l = x_1 + ix_2(1-\nu^2/c_l^2)^{1/2} \quad (11)$$

$$Q = 4(1-\nu^2/c_s^2)^{1/2} (1-\nu^2/c_l^2)^{1/2} - (2-\nu^2/c_s^2)^2$$

where  $c_l$  and  $c_s$  are the longitudinal and shear elastic wave speeds, respectively [18].

#### Results for Time-Independent Cohesive Stress

Detailed results on the initial curves and the caustic curves which are predicted on the basis of this model are given in [18]. For the line plastic zone model and small scale yielding conditions, it was found that the geometrical features of these curves are strikingly different from the curves corresponding to an elastic crack. For example, it was found that the initial curves were made up of two separate curves which were nested in some cases and were disjoint in other cases. These features of the initial curves gave rise to gaps, cusps, and other irregularities in the corresponding caustic curves.

The main result included here is the relationship between the observed size of the caustic curve and the value of the dynamic stress intensity factor inferred from that caustic and, in particular, the influence of crack tip plasticity on this relationship. For this discussion, suppose that the size of the caustic curve is determined by its maximum extent in the direction perpendicular to the direction of tensile crack growth. This size will be denoted by  $D$ . For a purely elastic tensile crack under quasi-static conditions the relationship

$$D = 2.593 \left( \frac{\nu z_0 d}{E} K_I \right)^{2/5} \quad (12)$$

is well known. The corresponding relationship for the case when both material inertia and crack tip plasticity effects are included in the model has been determined numerically, and the results are shown in nondimensional form in Fig. 4. The dashed

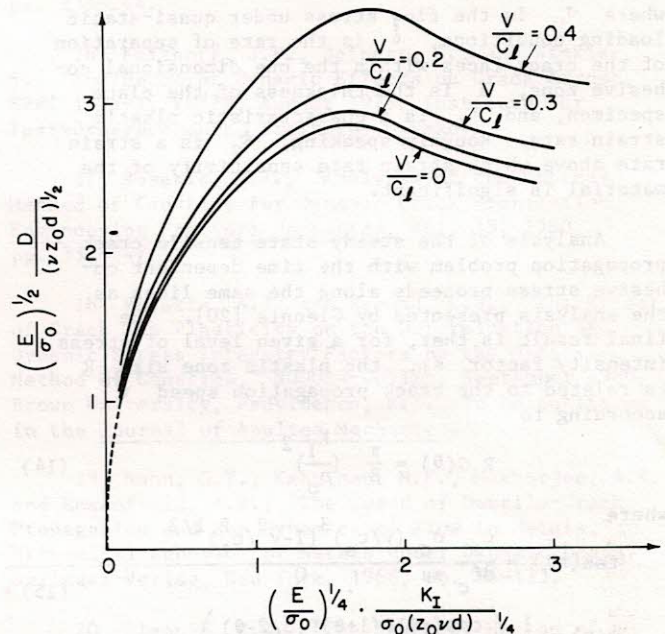


Fig. 4 The transverse diameter of the caustic curve  $D$  versus the remote elastic stress intensity factor,  $K_I$ , for four crack velocities

curve in Fig. 4 is simply a graph of equation (12) which is valid for  $v = 0$  and  $R = 0$ . As can be seen, the dashed curve fits very well with the computed results for  $v = 0$ . It would appear from Fig. 4 that if experimental observations are confined to situations for which  $(K_I/\sigma_0)(E/\sigma_0 \nu z_0 d)^{1/4}$  is less than about 1.0, then plasticity effects need not be taken into account in the interpretation of the observations. The possibility of adjusting the value of this nondimensional parameter simply by changing  $z_0$  is only apparent because, in any experimental setup, the distance  $z_0$  must be chosen so that the initial curve lies within a region of the specimen near the crack tip where the  $K$ -dominated small scale yielding solution accurately represents the stress field. It is also shown in [18] that the influence of inertia on the  $D$  versus  $K_I$  relationship is not large if  $v/c$  is less than about 0.20.

## Effect of a Strain Rate Dependent Cohesive Stress

As is indicated above, the determining factor in whether or not plasticity effects must be taken into account when interpreting caustics data is the size of the plastic zone compared to the extent of the initial curve on the specimen surface. In those materials in which the plastic flow stress depends on the rate of deformation, the size of the plastic zone will be a function of crack tip speed for any given stress intensity factor level. Therefore, in this section, the influence of rate sensitivity of the cohesive stress in the one dimensional plastic zone on the size of the plastic zone is considered. The assumption used previously by Hahn, et al. [19] and by Glennie [20] is adopted, according to which the cohesive stress within the plastic zone varies linearly with the separation rate in the plastic zone. The cohesive stress is given by

$$\sigma = \sigma_0(1 + \dot{\delta}/2d\dot{\epsilon}_c) \quad (13)$$

where  $\sigma_0$  is the flow stress under quasi-static loading conditions,  $\dot{\delta}$  is the rate of separation of the crack faces within the one dimensional cohesive zone,  $d$  is the thickness of the plate specimen, and  $\dot{\epsilon}_c$  is a characteristic plastic strain rate. Roughly speaking,  $\dot{\epsilon}_c$  is a strain rate above which strain rate sensitivity of the material is significant.

Analysis of the steady state tensile crack propagation problem with the time dependent cohesive stress proceeds along the same lines as the analysis presented by Glennie [20]. The final result is that, for a given level of stress intensity factor  $K_I$ , the plastic zone size  $R$  is related to the crack propagation speed  $v$  according to

$$R G(\theta) = \frac{\pi}{8} \left( \frac{K_I}{\sigma_0} \right)^2 \quad (14)$$

where

$$\tan(\pi\theta) = \frac{c_s \sigma_0}{d \dot{\epsilon}_c \pi \mu} \frac{(v/c_s)^3 (1-v^2/c_l^2)^{1/2}}{Q} \quad (15)$$

$$G(\theta) = \frac{1}{\pi} \left( \frac{\cos(\pi\theta) \Gamma(1+\theta) \Gamma(3/2-\theta)}{\Gamma(\theta-1/2)} \right)$$

The symbol  $\Gamma$  in (15) represents the gamma function. The relationship (14) has been evaluated numerically, and the results are shown in Fig. 5 for three values of the characteristic strain rate  $\dot{\epsilon}_c$ . For the calculations,  $c_s = 3200$  m/s,  $c_l = 6000$  m/s,  $d = 1$  cm and  $\sigma_0/\mu = 10^{-3}$ . It is clear from this figure that the plastic zone size is quite sensitive to crack propagation speed at a given level of stress intensity factor. Of course, the level of stress intensity factor required to sustain crack propagation is also a function of crack speed for most materials. For materials for which the stress intensity factor required to sustain crack growth is an increasing function of crack speed, the two effects tend to cancel each other. That is, at increasing speeds, the increase in the  $K_I$  level tends to increase the plastic zone size while the strain rate sensitivity tends to decrease the plastic zone size. The net effect can be determined only in light of specific data.

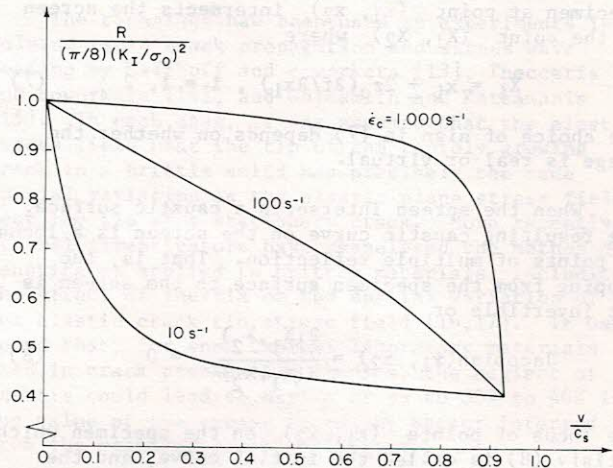


Fig.5 Plastic zone size  $R$  versus crack speed for three values of critical strain rate

## CONCLUDING REMARKS

The experimental procedure for the determination of the influence of loading rate on fracture initiation resistance of materials has been applied successfully for three steels. It should be noted that this method has both advantages and disadvantages. The main advantage is that the rate of loading is very rapid with  $K_I = 10^6$  MPa $\sqrt{m/s}$ , comparable to rates achieved in impact tests, and yet the instrumentation provides accurate and unambiguous measures of crack opening displacement and average stress on the fracturing section. The main disadvantage of the procedure, when compared to a standard test like the Charpy test, is that the specimens are expensive to produce and instrument. Furthermore, the method requires the prior growth of a circumferential fatigue crack at the root of the notch. Because a concentric crack can be grown only in transversely isotropic materials, the method generally is limited to bar stock. The use of explosives to produce the dynamic loads may be regarded as an advantage or disadvantage, depending on the available laboratory facilities. In any case, this same test may be performed without explosives by producing the tensile loading pulse through impact.

The measurement of crack tip deformations during rapid crack propagation by means of the optical method of caustics has been established as a standard procedure for transparent materials, and the use of the technique with reflected light holds promise for testing opaque structural materials. The main advantage of a direct crack tip measurement is that the interpretation of data does not rely on a transient stress analysis of the entire specimen. A disadvantage of the method is that it provides surface measurements and, thus, interpretation of the data rests on the assumption that the three dimensional surface effects observed are uniquely linked to the essentially two dimensional conditions which

prevail in the interior of the specimen. An analysis which applies for the situation of a growing crack intersecting the free surface of a plate specimen is not yet available. However, analyses of elastic-plastic crack growth under nominally plane stress conditions are available in the literature, and interpretation of caustics data obtained in reflection is being pursued on the basis of these analyses.

#### ACKNOWLEDGEMENTS

The research support of the Office of Naval Research, Structural Mechanics Program, Grant N00014-78-C-0051, and the NSF Materials Research Laboratory at Brown University is gratefully acknowledged.

#### REFERENCES

- 1 Krafft, J.M. and Irwin, G.R., Crack-Velocity Considerations," Fracture Toughness Testing and Its Applications, American Society for Testing and Materials, STP 381, 1965, pp. 114-129.
- 2 Costin, L.S., Duffy, J., and Freund, L.B., "Fracture Initiation in Metals under Stress Wave Loading Conditions," Fast Fracture and Crack Arrest, American Society for Testing and Materials, STP 627, 1977, pp. 301-318.
- 3 Kolsky, H., "An Investigation of the Mechanical Properties of Materials at Very High Rates of Loading," Proceedings of the Physical Society London, Vol. 62-B, 1949, pp. 676-700.
- 4 Tada, H., The Stress Analysis of Cracks Handbook, Del Research Corporation, 1973, Hellertown, Pennsylvania.
- 5 Duffy, J., Campbell, J.D., and Hawley, R.H., "On the Use of a Torsional Split Hopkinson Bar to Study Rate Effects in 1100-0 Aluminum," Journal of Applied Mechanics, Vol. 38, March, 1971, pp. 83-91.
- 6 Paris, P.C., written discussion of J.A. Begley and J.D. Landes, "The J-Integral Integral as a Fracture Criterion," Fracture Toughness, American Society for Testing and Materials, STP 514, 1972, pp. 1-23,
- 7 Rice, J.R., Paris, P.C., and Merkle, J.C., "Some Further Results of J-Integral Analysis and Estimates," Progress in Flaw Growth and Fracture Toughness Testing, American Society for Testing and Materials, STP 536, 1973, pp. 231-245.
- 8 Hutchinson, J.W. and Paris, P.C., "Stability Analysis of J-Controlled Crack Growth," Elastic-Plastic Fracture, American Society for Testing and Materials, STP 668, 1979, pp. 37-64.
- 9 Costin, L.S. and Duffy, J., "The Effect of Loading Rate and Temperature on the Initiation of Fracture in a Mild, Rate-Sensitive Steel," Journal of Engineering Materials and Technology, Vol. 101, July 1979, pp. 258-263.
- 10 Wilson, M.L., Hawley, R.H., and Duffy, J., "The Effect of Loading Rate and Temperature on Fracture Initiation in 1020 Hot-Rolled Steel," Engineering Fracture Mechanics, Vol. 13, 1980, pp. 371-385.
- 11 Costin, L.S., "The Effect of Loading Rate and Temperature on the Initiation of Fracture in a Mild Rate-Sensitive Steel," NSF ENG77-08897/2, May 1978, Brown University, Providence, R.I.
- 12 Manogg, P., "Anwendung der Schattenoptik zur Untersuchung des ZerreiBsvorganges von Platten," Dissertationsschrift, 1964, an der Universität Freiburg, Germany.
- 13 Kalthoff, J.F., Winkler, S. and Beinert, J., "Dynamic Stress Intensity Factors for Arresting Cracks in DCB Specimens," International Journal of Fracture, Vol. 12, 1976, pp. 317-319.
- 14 Theocaris, P.S., "Local Yielding Around a Crack Tip in Plexiglass," Journal of Applied Mechanics, Vol. 37, June 1970, pp. 409-415.
- 15 Goldsmith, W. and Katsamanis, F., "Fracture of Notched Polymeric Beams Due to Central Impact," Experimental Mechanics, Vol. 19, July 1979, pp. 235-244.
- 16 Kalthoff, J.F., Beinert, J., and Winkler, S., "Influence of Dynamic Effects on Crack Arrest," EPRI 1022-1, V9/78, August 1978, Institute für Festkörpermechanik, Freiburg, Germany.
- 17 Rosakis, A.J., "Analysis of the Optical Method of Caustics for Dynamic Crack Propagation," Engineering Fracture Mechanics, Vol. 13, 1980, pp. 331-347.
- 18 Rosakis, A.J. and Freund, L.B., "The Effect of Crack Tip Plasticity on the Determination of Dynamic Stress Intensity Factors by the Optical Method of Caustics," N00014-0051/5, September 1980, Brown University, Providence, R.I. To be published in the Journal of Applied Mechanics.
- 19 Hahn, G.T., Kanninen, M.F., Mukherjee, A.K., and Rosenfield, A.R., "The Speed of Ductile-Crack Propagation and the Dynamics of Flow in Metals," Mechanical Behavior of Metals under Dynamic Loads, Springer-Verlag, New York, 1968, pp. 96-133.
- 20 Glennie, E.B., "The Unsteady Motion of a Rate-Dependent Crack Model," The Journal of the Mechanics and Physics of Solids, Vol. 19, 1971, pp. 329-338.